Designing and Harnessing the Metastable States of a Modular Metastructure for Programmable Mechanical Properties Adaptation

R. L. Harne[1]
Department of Mechanical and Aerospace Engineering,
The Ohio State University,
Columbus, OH 43210
e-mail: harne.3@osu.edu

Z. Wu
Department of Mechanical Engineering,
University of Michigan,
Ann Arbor, MI 48109

K. W. Wang
Department of Mechanical Engineering,
University of Michigan,
Ann Arbor, MI 48109

Recent studies on periodic metamaterial systems have shown that remarkable properties adaptivity and versatility are often the products of exploiting internal, coexisting metastable states. Motivated by this concept, this research develops and explores a local-global design framework wherein macroscopic system-level properties are sought according to a strategic periodic constituent composition and assembly. To this end and taking inspiration from recent insights in studies of multiphase composite materials and cytoskeletal actin networks, this study develops adaptable metastable modules *that are assembled into* modular metastructures*, such that the latter are invested with synergistic features due to the strategic module development and integration. Using this approach, it is seen that modularity creates an accessible pathway to exploit metastable states for programmable metastructure adaptivity, including a near-continuous variation of mechanical properties or stable topologies and adjustable hysteresis. A model is developed to understand the source of the synergistic characteristics, and theoretical findings are found to be in good agreement with experimental results. Important design-based questions are raised regarding the modular metastructure concept, and a genetic algorithm (GA) routine is developed to elucidate the sensitivities of the properties variation with respect to the statistics amongst assembled module design variables. To obtain target multifunctionality and adaptivity, the routine discovers that particular degrees and types of modular heterogeneity are required. Future realizations of modular metastructures are discussed to illustrate the extensibility of the design concept and broad application base.*
[DOI: 10.1115/1.4032093]

1 Introduction and Motivations

Materials and structures invested with adaptivity more effectively interact with a wide range of environmental variations and operating conditions. Such system-level multifunctionality can help minimize weight and maximize suitability to diverse missions and maneuvers, factors which are favorable, for example, in aerospace, automotive, and defense industries [1]. Metamaterials are one example of material systems achieving such valuable features. By periodic, cellular, and even origami-inspired designs, the global (macroscopic) properties of metamaterials have included tunable Poisson's ratio [2,3], drastic topological change [4], inverted compressibility [5], selective wave steering and resonance tuning [6,7], and more. According to the operating states, such properties may or may not be activated, leading to controllable reaction force [8,9] and elastic wave propagation capacity [10,11], among other characteristics.

A recurring theme in the recent studies is the advantage provided by coexisting metastable states (sometimes termed multistability), since they often facilitate property changes without the need for continuous, active control intervention. Exemplary demonstrations of the adaptivity enabled by multiple stable states include the morphing capabilities of prestressed composite laminates [12,13] or origami-inspired designs [14–16], such that the system topology may dramatically vary between the statically stable shapes.

2 Research Objectives

Recently, the authors have created and explored a concept based on adaptable mechanical modules, invested with means to change macroscopic characteristics by switching among the available metastable states [17], for instance switching via direct actuation. These building blocks employ the fundamental constituents required to effect metastable states: positive and negative stiffness springs in series, a requirement determined previously from investigations of multiphase composites [18,19] and cytoskeletal actin networks [20]. Using such *metastable modules*, the authors have given first evidence of a large growth of system-level adaptivity by the parallel assembly of these building blocks into *modular metastructures*, where the latter term is used to denote the synergy of the whole resulting from the assembly of the constituents [17]. Due to the particular module design, the extent of the prior studies was limited to two, assembled metastable modules, although this was sufficient to result in several statically stable topologies, means for properties adaptation, and hysteretic damping capacity driven by reversible, passive state switching under near quasi-static loading scenarios [17].

The objective of this research is to build upon the authors' foundational concept by redesigning the mechanical module in such a way as to investigate how the favorable system-level adaptivity and performance of modular metastructures should be tailored with the assembly of *many* metastable modules. In so doing, this presents the opportunity to explore how to best *design* such

[1]Corresponding author.

Contributed by the Design Automation Committee of ASME for publication in the Journal of Mechanical Design. Manuscript received June 25, 2015; final manuscript received October 27, 2015; published online December 10, 2015. Assoc. Editor: James K. Guest.

modular metastructures for a given set of targeted macroscopic characteristics. Thus, this research begins to establish a new local–global design framework whereby the local modules are designed such that a targeted global synergy is effected once the modules are assembled into modular metastructures. In the process of exploring this local-global framework, answers to several design-based questions are sought. These questions include (i) what degree of parametric heterogeneity is permissible or desirable toward realizing the target adaptivity performance, (ii) what types of heterogeneity are to be considered, and (iii) are such conclusions extensible to metastructures composed of any number of metastable modules?

To accomplish the research objective and explore the local-global design framework, a series of tasks are performed and discussed in the following sections. In Sec. 3, the experimental module created to facilitate the assembly of many such modules into metastructures is introduced, and gives evidence that the product of this design strategy may be a remarkable synergy at the macroscopic level. In Sec. 4, a theoretical study provides insights to the qualitative persistence and evolution of metastable states and property adaptivity. In Sec. 5, additional experimental evaluations elucidate how modularity can be exploited to invest metastructures with direct means for massive property change such as reaction force variation and tunable hysteresis. In Sec. 6, a GA routine is developed and investigated to probe the parametric sensitivities exhibited with respect to achieving specific properties adaptivity goals, thus establishing rational means to *locally* design the metastable states of modules to realize targeted *global* metastructure performance once the modules are thereafter assembled.

3 Experimental Module, Assembly Strategy, and Exemplary Properties Adaptivity

Prior researchers have shown that inducing coexisting metastable states in mechanical systems is fundamentally accomplished using a bistable (negative stiffness) spring in series with a positive stiffness spring [18–20], Fig. 1(*a*). Properly designed, the two, local minima of potential energy of the bistable component enables the *module* to possess two metastable states, whereby the macroscopic topology, z in Fig. 1(*a*), remains the same while the reaction force F_i (and related properties such as stiffness) may be adapted. A module employing a bistable spring alone is insufficient to induce *coexisting* metastable states because the additional positive stiffness series spring introduces the means to equalize the macroscopic load at two coexisting internal configurations, which is the essential adaptation mechanism [18]. In this study, building upon the authors' prior study of assembling two such archetypal metastable modules together [17], a new one-dimensional metastable module is created and investigated so as to facilitate the assembly of *many* modules together into metastructures. This enables the evaluation of how the macroscopic properties of the *metastructure* are tailored due to the design and switching among the many metastable states, as sketched in Fig. 1(*b*).

A schematic of the new module created here is given in Fig. 1(*c*). The essential components for effecting metastable states are retained: a bistable spring in series with a positive stiffness spring. The bistable spring is generated by geometric constraints: four spring steel beams are bonded between an acrylic/PMMA housing and shuttle such that the distance between the housing and shuttle ($\delta \approx 13$ mm) is less than the beam lengths prior to bonding ($\ell \approx 14$ mm). In series with the bistable spring is a spring that connects the bistable shuttle, displaced by x, to the PMMA facing element which is acted upon by the end displacement z. This series spring force is due to tensioned elastic bands that interface the shuttle and facing components. Parallel assemblies are created by stacking and constraining the modules at the housing ends using alignment rods while a common, rigid guide rod governs the resulting metastructure end displacement z, as shown in Fig. 1(*c*). Photographs of one experimental proof-of-concept module and multimodule metastructure assembly are given in Figs. 1(*c*) and 1(*d*), respectively.

Experiments are undertaken with the housing ends of assembled modules secured to an optical table (Newport RS 3000) while the guiding end displacements z are governed by a motion controller/stage system (Newport IMS500CC) moving at a rate of 100 μm/s with displacement resolution of 1.25 μm. The same experimental routine applies whether capturing data for an individual module or for a multimodule metastructure. Measurements are taken for the one-dimensional end displacement z using a potentiometer (Novotechnik TR-100) and for the resulting reaction force F using a load cell (Measurement Specialties ELAF-TIE-100L) at the end displacement location. The load cell measurements pass through an analog, fourth-order low-pass Butterworth filter (DL Instruments 4302) at 10 Hz at the point of acquisition while all data are postprocessed using a digital, second-order low-pass Butterworth filter at 1 Hz.

To first evaluate the efficacy of the new module design toward realizing coexisting metastable states and possibility for adaptivity growth in metastructure assemblies, experiments are conducted using the methods detailed above for an individual module, and then for metastructures assembled from two, four, and six

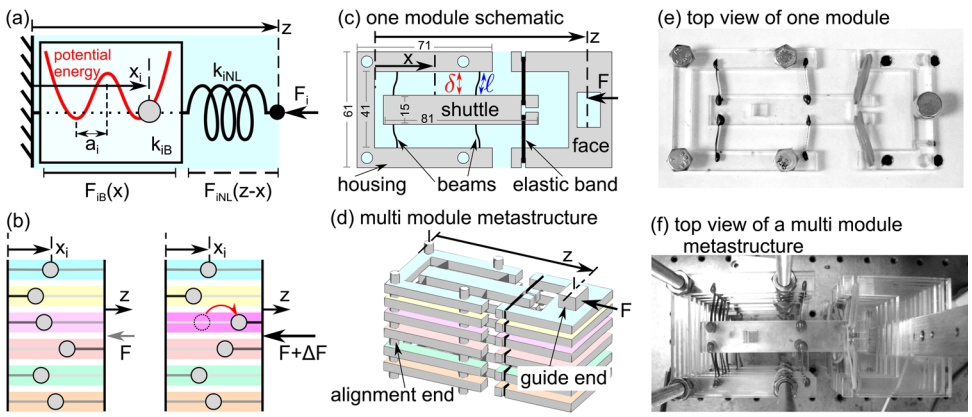

Fig. 1 (*a*) Model schematic of bistable spring (double-well potential energy profile) in series with positive stiffness spring acted upon by end displacement. (*b*) Illustration of reaction force *F* adaptation when a one metastable module of a multimodule metastructure transitions from one to another metastable state: the force is modified to $F + \Delta F$ while end displacement *z* is constant. (*c*) Schematic of experimental, mechanical metastable module. Dimensions are given in mm. (*d*) Schematic of multimodule metastructure assembly and experimental implementation. (*e*) Top view photograph of one experimental module and (*f*) a multimodule metastructure.

modules in parallel. Figure 2 presents exemplary measurements of normalized reaction force as the end displacement is varied quasi-statically. Each curve indicates a metastable state; when multiple states are discovered, multiple experiments are conducted to measure them all. To measure each state, data collection is begun at an end displacement approximately halfway along the full range considered and then two measurements are taken where one involves reducing end displacement values and the other uses increasing end displacements from this interior starting point. The reaction force normalization used in plotting is with respect to the largest absolute force measured for the six module metastructure, which occurs around an end displacement $z = 22$ mm.

For the individual module results shown in the top panel of Fig. 2, over a range of end displacements there are two coexisting metastable states that induce unique macroscopic mechanical properties. In other words, for topologically identical end displacements, the module may provide two distinct reaction forces. The metastable module design investigated here therefore meets the requirements for properties adaptation by effecting such necessary metastable states. Then, Fig. 2 shows that modular metastructures of increasing number of modules produce a massive increase in the number of possible coexisting metastable states. In spite of a significant heterogeneity from module-to-module, the measurements uncover 4, 16, and then 64 coexisting metastable states for the two, four, to six module metastructures, respectively, which suggests that heterogeneity may play an important role to realize the many coexisting states. The consequence of the many metastable states is that near-continuous properties adaptivity is effected for particular macroscopic topologies. For example, the bottom panel of Fig. 2 shows that around 8 mm end displacement for the six module metastructure, the reaction force may be tailored amongst an enormous number of values spanning the range from about −0.08 to 0.11 normalized force. As Fig. 1(*d*) illustrates, the effort required to achieve such properties adaptation is the switching of internal metastable states amongst the assembled modules from initial to desired, final states/properties. Once the final state is realized, no additional active effort is needed to maintain the new macroscopic property unlike many active materials that require persistent electrical, temperature, or other interventions to sustain the tailored property. In addition, for these examples Fig. 2 shows that each module and modular assembly effects more than one stable equilibrium (zero reaction force), which is a statically stable shape. The bottom panel of Fig. 2 shows that the large number of metastable states and stable topologies for the six module metastructure gives rise to near-continuous stable shape change over a certain displacement range. In contrast to zero-stiffness structures that undergo large free displacements due to a lack of restoring forces [21], the modular metastructures retain viable stiffness at each stable topology, providing a means to "lock" in shape once the new stable form is realized. In a way, this property is similar to a reversible plasticity [22] realized using a strategic combination of elastic constituents. These results exemplify that effective module design—providing coexisting metastable states—leads to exceptional, synergistic properties adaptivity on the metastructural scale following strategic assembly, justifying the design concept and motivating closer investigation.

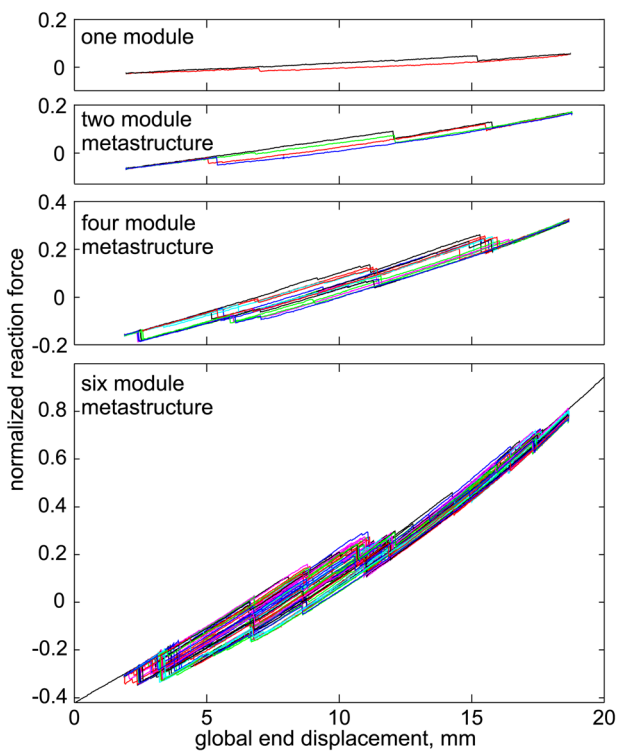

Fig. 2 Normalized experimental reaction force as end displacement is varied. From top to bottom panels, measurements of one module, and then of two-, four-, and six-module metastructures. Each curve is a metastable state.

4 Theoretical Formulation and Study

An analytical model of modular metastructures is formulated to verify and validate the intriguing experimental trends and, in Sec. 6, to explore characteristics of the metastructure design concept not currently accessible via the experimentation. For the *i*th module of an n module metastructure, the bistable spring force is approximated using $F_{iB} = k_{iB}x_i(x_i - a_i)(x_i - 2a_i)$ where the displacement of the shuttle is x_i, the stiffness coefficient is k_{iB}, and the distance between the stable equilibria is $2a_i$, denoting the "span" by a_i as the distance between one stable equilibrium and the central unstable internal configuration. Although this is an inexact expression for the true spring force exhibited between the guided-fixed beams and the shuttle, the cubic polynomial formulation is still qualitatively comparable to the exact profile [23] and usefully enables an analytical determination of the numerous metastable, force–displacement profiles without the need for nonlinear equation solvers or finite element modeling [24]. The forces exerted in the axis of end displacement by deforming the elastic bands are purely nonlinear [25], and are expressed using $F_{iNL} = k_{iNL}(z - x_i)^3$. The macroscopic mechanical properties of metastructures are determined by first consolidating the constituent potential energy contributions. The total potential energy of an n module metastructure is

$$U = \sum_{i=1}^{n}\left[a_i^2 k_{iB}x_i^2 - a_i k_{iB}x_i^3 + \frac{1}{4}k_{iB}x_i^4 + \frac{1}{4}k_{iNL}(z + d_i - x_i)^3\right] \quad (1)$$

where d_i is an attachment offset distance that accounts for inevitable deviations of total module length from one module to another with respect to the common, guiding end displacement and reference attachment location. In the experimental realizations, the offset distances of an n module metastructure are seen to exhibit a small standard deviation around a near-zero mean distance value since the modules each vary slightly in total length and it is desired to reference the end displacement at approximately the point of the mean total length. By the parallel assembly approach when the end displacement z is fixed, the expressions for stable configurations are decoupled. In this way, static equilibria satisfy the system of equations $\partial U/\partial x_i = 0$ $(i = 1, 2, \ldots, n)$, whereas stable equilibria are those which also satisfy $\partial^2 U/\partial x_i^2 > 0$ $(i = 1, 2, \ldots, n)$ [22]. Consequently, the net reaction force measured at the global end of the n module metastructure is $F = \sum_{i=1}^{n} k_{iNL}(z + d_i - x_i)^3$. Due to the parallel assembly strategy considered here, the n equations given by $\partial U/\partial x_i = 0$ are decoupled, algebraic polynomial equations, which enables the direct solution of the possible metastable states x_i of an n module metastructure, and thereafter the macroscopic reaction force F.

From the top to bottom panels, Fig. 3 presents exemplary analytical results of the normalized reaction force F as the end displacement z is varied quasi-statically for an individual module, and then for two, four, and six module metastructures, respectively. To compute these results, the bistable spring stiffness coefficient values k_{iB} and span distances a_i are arbitrarily selected ($k_{iB} = 2\,\mathrm{N{\cdot}m^{-3}}$, $a_i = 0.5\,\mathrm{m}$) so as to emulate the qualitative trends of the measurements for the sake of illustration. The remaining coefficients include notable heterogeneity. Specifically, stiffness coefficients k_{iNL} are randomly selected from a normal distribution of values having standard deviation of $1\,\mathrm{N{\cdot}m^{-3}}$ and mean of $0.6\,\mathrm{N{\cdot}m^{-3}}$; the attachment offset distances d_i are likewise randomly selected where standard deviation is 0.07 m and mean is 0 m. For a given module, these random variations influence the extent of end displacements across which coexisting metastable states occur [17] which is the most apparent distinguishing factor among fabricated modules once assembled.

The trends observed in Fig. 3 are in overall good qualitative agreement to the measurements in Fig. 2 with respect to the exponential growth of the total number of coexisting metastable states as greater numbers of modules are assembled together. For theoretical exploration purposes at the current phase of concept development, this level of agreement is sufficient; future model formulations of the current platform may account for the precise bistable spring behavior which is slightly more intricate that the cubic polynomial expression employed here [23]. According to the theory, at most 2^n coexisting states are possible for an n module metastructure. Indeed, the analytical results show that the growth of the total number of metastable states is robust to the appreciable heterogeneity applied via coefficient perturbations from nominal values. Comparable to measurements, the bottom panel of Fig. 3 shows that a metastructure assembled from six modules effects a capability for near-continuous mechanical properties adaptivity and shape change, both over a given extent of values. These features are specifically enabled by the modularity

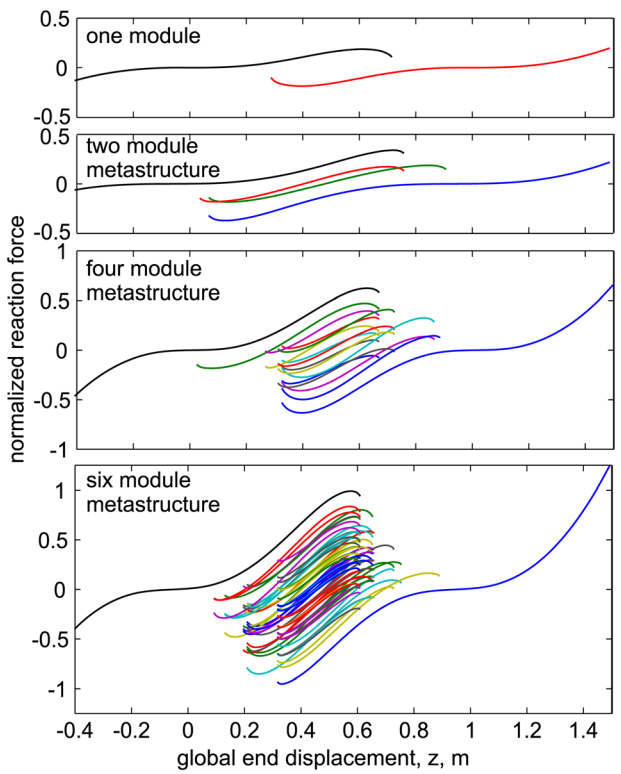

Fig. 3 Theoretical predictions of normalized reaction force *F* as end displacement z is varied. From top to bottom panels, results for one module, and then of two-, four-, and six-module metastructures. Each curve is a metastable state.

of the system. In contrast with periodic metamaterial systems which may possess large multistability but have limited means to exploit or explicitly realize the various states to tailor properties, modular metastructures (composed of even only a few modules) facilitate the direct creation of a vast number of metastable states that represent unique mechanical properties useful for adaptation purposes. It is clear that by developing a suitable module possessed with coexisting metastable states, the assembly of such constituents promotes a synergistic growth of structural adaptivity, even accounting for considerable parametric heterogeneity.

5 Harnessing Transitions Among Metastable States for Properties Adaptation

Enormous properties adaptivity and stable shape change are desirable features for many advanced engineering systems, including for morphing aircraft [26] and for structures with dramatic dynamics-based energy transfer features [27,28]. Beyond the favorable static characteristics of the modular metastructures exhibited in Sec. 3, here experiments are conducted by subjecting a six module metastructure to slow, periodic excitation to explore intelligent passive-adaptation capabilities in response to time-varying external influences. For example, such valuable transformations include maintaining a constant global topology while an applied force changes or maintaining a constant reaction force while an applied end displacement is varied.

To illustrate the prior, Fig. 4(*a*) plots the reactions forces from 13 trials of transitioning an experimental six-module metastructure from a common initial metastable state (0-0-1-0-1-0) to a common final state (1-0-0-1-0-1), where 0s and 1s indicate the bistable springs are buckled away from or toward the facing ends, respectively. The experiments are conducted by maintaining an 8 mm end displacement while sequential, manual actuations (by direct point force application) upon the shuttles induce switches amongst internal configurations, and hence amongst global macroscopic properties. For example, one experiment follows the transition series (0-0-1-0-1-0), (0-0-1-0-0-0), (0-0-0-0-0-0), (0-0-0-1-0-0), and so on until the state (1-0-0-1-0-1). The unique plotted curves, Fig. 4(*a*), are therefore the reaction forces generated for 13 different trials of transitions from common initial to common final states, and therefore common reaction forces. The curve shading from light to dark indicates increasing mean value of force with respect to the 13 trials. Reaction forces are normalized to initial common values, while time is normalized according to the number of discrete, sequential transitions. For these experiments, five discrete transitions are executed, leading to six stages for each trial.

The results in Fig. 4(*a*) make clear that modularity invests a significant opportunity for reacting to applied forces in unique ways that maintain global metastructure topology. In this example, transitioning from common initial to common final reaction forces may be undertaken using an enormous number of possible series of reaction force variations. Thus, considering the applied force conditions with respect to maintaining a desired global topology, an appropriate transition series may be selected. For instance, an increasing/decreasing applied force may be best reacted to using the transition series shown as the darkest curve, whereas a decreasing/increasing applied force may be best reacted against using the lightest curve transition path. In this way, the metastructure may most effectively adapt to different environment loading conditions while the global topology is fixed. Indeed, assessing the combinatorics of the permutations [29], the number of possible adaptable transition series for metastructures undergoing g discrete transitions from common initial to common final reaction forces is $g!$ (here, $5! = 120$).

When the end displacement of the metastructure is guided periodically, the resulting loops of hysteresis are found to be unique based upon the switches in state that are effected due to loss of stability from one metastable state to the next. The measurements in Fig. 4(*b*) from a six-module metastructure exemplify the case

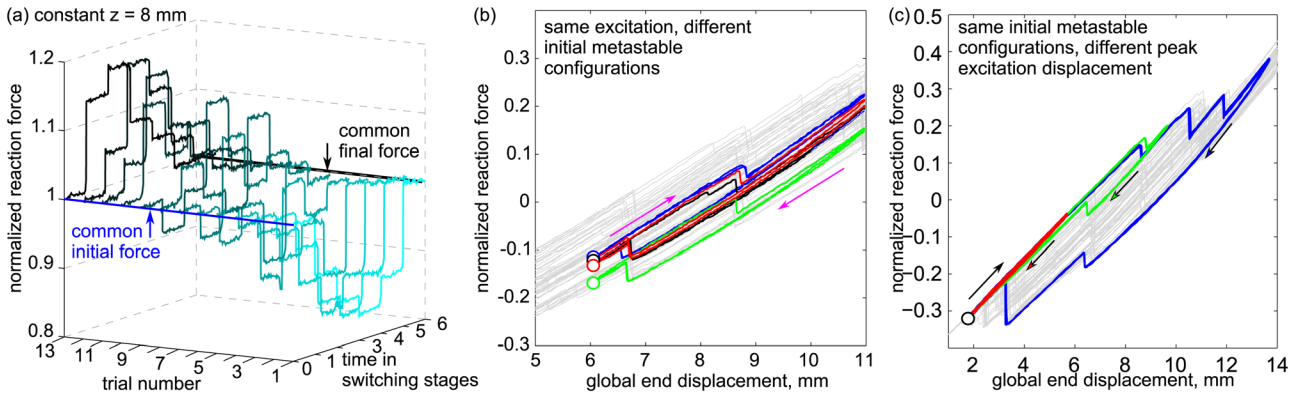

Fig. 4 Experimental measurements. (*a*) Transitioning a six module metastructure from common initial to common final states via different orders of transitions. Light to dark line shading indicates increasing mean value of reaction force with respect to all trials. (*b*) Distinct hysteresis loops having common minimum and maximum global end displacements, but unique sets of metastable states throughout slow actuation cycles. (*c*) Distinct hysteresis loops having common starting end displacement but qualitatively distinct unloading paths due to different maximum end displacement. In (*b*) and (*c*), background gray curves are quasi-static reaction force measurements; thick curves (colored) show two cycles of data, indicating repeatability to the measurements; circles indicate starting points.

in which the same loading and unloading end displacement is prescribed but different starting sets of internal metastable configurations lead to different hysteresis over the course of the slow (near quasi-static) actuation cycle. In this example, the measurements begin for an end displacement near 6 mm (circle points). During the slow actuation cycles, distinct, steady-state hysteresis loops are uncovered, four of which are shown in Fig. 4(*b*) by the thick curves plotted over the thin, light gray plot of the static measurements of the six-module metastructure mechanical properties (previously given in Fig. 2). The hysteresis loops are seen to vary in terms of the energy loss per cycle (area enclosed in the Lissajous curves) as well as in terms of the mean value of reaction force, which extends the properties adaptivity potential of recent advancements in metamaterials [8]. Thus, by exploiting these "hidden" degrees-of-freedom [30], the macroscopically observable hysteresis of the metastructure may be leveraged in novel ways.

Figure 4(*c*) presents measurements when the six-module metastructure is slowly actuated by an end displacement starting near 2 mm. Different amplitudes of actuation are applied from the common starting position, before the unloading half cycle. The results show that the coexistence of many metastable states leads to distinct hysteresis based upon which internal transitions are induced during the cyclic loading. Thus, rather than rely solely upon conventional damping mechanisms such as Joule heating to dissipate the cyclic, actuation energies, the modular metastructures leverage a feature similar to a "reversible plasticity" wherein the internal instabilities promote tunable energy decay to "high frequency (dissipative) modes" even in the near quasi-static actuation scenario [22]. Comparable phenomena are observed in the experiments when metastructures are actuated starting from different initial end displacements. Collectively, enormous and adjustable hysteresis is effected based upon the initial end displacement and initial metastable state. Moreover, in spite of the considerable heterogeneity in the experimental metastructures, it is worth highlighting that the results in Figs. 4(*b*) and 4(*c*) overlay two cycles of measurements which shows that the adaptable characteristics are repeatable and consistent.

6 Design of Multimodule Metastructures

The results shown in Secs. 3–5 indicate that the static and quasi-static characteristics of modular, mechanical metastructures exhibit enormous potential for adaptivity. Even in this conceptual phase of development, questions could be raised as to the viability of realizing many metastable states that yield desirable property adaptation. For example, to "program" the desired adaptivity feature or its level in this local-global design framework, (i) what *degree* of parametric heterogeneity is permissible and/or desirable, (ii) what *types* of heterogeneity are permissible, and (iii) are these conclusions consistent for multimodule metastructures of any number of assembled modules? In the face of near open-ended opportunity for parameter selection, a design methodology is needed to take this structural/material assembly concept beyond a seminal phase.

To explore these parametric influences, a GA is devised based upon the analytical model foundation. According to the formulation, the model uses the most reduced set of design variables possible to describe the salient factors that govern the macroscopic properties of the metastable modules: the bistable spring span a_i, the stiffness of the bistable, and attachment springs, k_{iB} and k_{iNL}, respectively, and the attachment offset distance d_i. The GA is first composed to evaluate and optimize performance measures by manipulating and evolving the bistable spring stiffness k_{iB} and span a_i design variables over the course of 50 generations each having a population of 100 individuals, where an individual is a six module metastructure. The algorithm is developed in-house and is devised upon an architecture described by Haupt and Haupt [31]. From one generation to the next, the selection/retention rate is 50% and the mutation rate is 20%, which together promote an aggressive search protocol useful for performance planes that exhibit multiple local minima.

6.1 Designing Metastructures With Equidistant Stable Equilibria. Two, prominent adaptivity characteristics were uncovered in Secs. 3 and 4 regarding multimodule metastructures: near-continuous change of stable topologies while reaction force is zero, or near-continuous change in reaction force while the global end displacement topology is prescribed. Therefore, the GA is programed to optimize relevant features of these adaptivity characteristics. In the following example, the first performance measure considered is the achievement of an equal spacing between adjacent statically stable equilibria of the six module metastructure, as illustrated in the top left panel of Fig. 5. Thus, a metastructure with the best "fitness" possible would have exactly equidistant adjacent stable equilibria (e.g., with stable equilibria locations at αj, where α is the spacing distance and $j = 1, 2, \ldots$). Since each of the six modules possess stiffness and span parameters, this suggests that 12 design variables are required to evaluate this performance measure using the GA. To circumvent difficulties encountered with GAs using many free variables, a novel *statistical* approach of GA utilization is undertaken here. Thus,

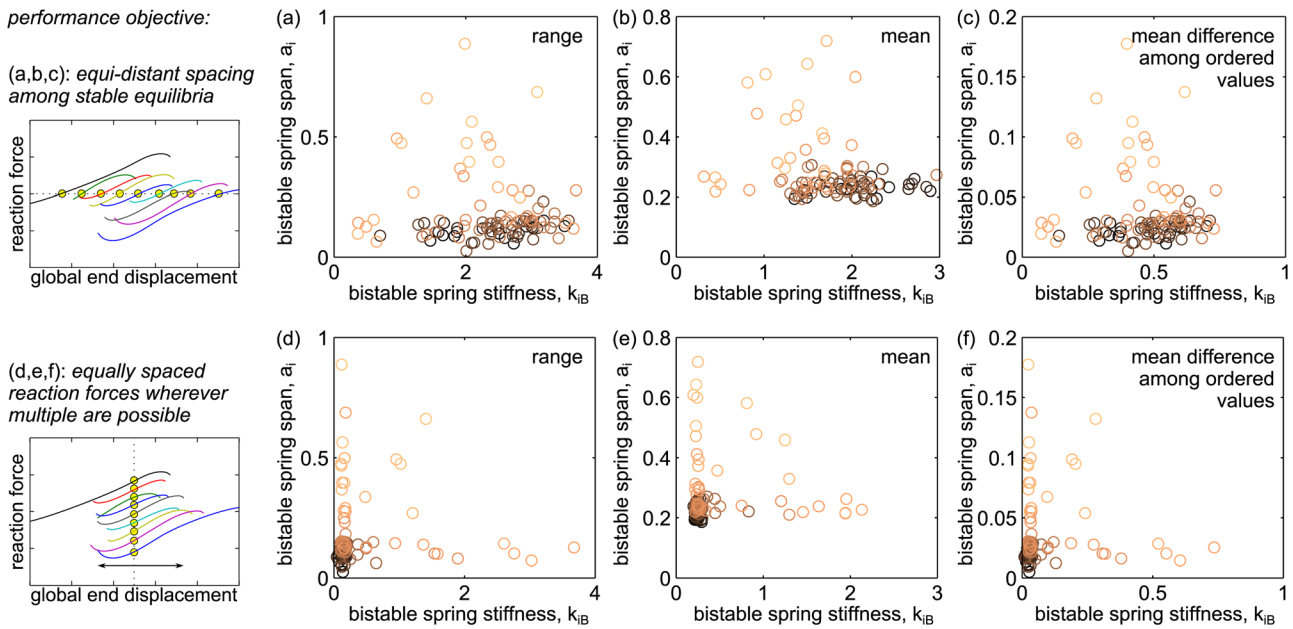

Fig. 5 In (*a*)–(*c*), the performance objective is equidistant spacing among stable equilibria of a given six-module metastructure. In (*d*)–(*f*), the objective is equally spaced reaction forces while the global end displacement is fixed. The left-most panels illustrate the performance objectives according to the particular mechanical properties shown as circle points on the full profiles. In (*a*)–(*f*), design variable statistics of all 100 individuals in the final generation produced by the GA. Shading from light to dark shows increasing fitness toward achieving the performance objective. (*a*) and (*d*) Range, (*b*) and (*e*) mean, and (*c*) and (*f*) mean difference among the ordered design variable values as plotted in terms of the bistable spring stiffness and bistable spring span.

a large range of permissible values are initially prescribed for the selection of k_{iB} and a_i, but, for a given module, the precise parameter value is selected at random within the range. By this modification to traditional GAs, it is recognized that complete convergence is not ensured. On the other hand, the findings presented below show that important design-based knowledge emerges from the *statistics* of the steadily convergent results.

Figure 6 presents the results of the GA toward achieving six-module metastructure designs having equally spaced adjacent statically stable equilibria. Each data point in Fig. 6 is the statistic with respect to the mean value for all individuals of the generation (triangles) or the value computed for the best-fit individual of the generation (circles). Note that because each *individual* is a six-module metastructure, each individual has a set of six bistable spring stiffnesses and six spring spans, and thus yields statistics that characterize those parameter value distributions. The top row shows how the *mean* value of the six Fig. 6(*a*) bistable spring stiffnesses and Fig. 6(*b*) bistable spring spans relatively converge over the course of the GA routine. It is seen that the generation means of the mean bistable spring span values, Fig. 6(*b*), converge toward a value around 0.28 m while the best-fit individual means converge toward a slightly smaller value nearer to 0.23 m. Together, these trends demonstrate the importance of appropriate selection of span values toward achieving equally spaced stable equilibria. In contrast, while the generation means of the bistable spring stiffness values, Fig. 6(*a*), converge to around 1.7 N/m^3, the best-fit individual mean values are seen to vary considerably from one generation to the next. Such low correlation between the convergence of the mean values for the whole generation of individuals and the mean value represented by the best-fit individual indicates that the bistable spring stiffness plays little role toward successfully meeting the target performance measure of equidistant stable equilibria. The fact that the generation mean itself converges simply illustrates a conventional fact of statistics that large, randomly selected variables from uniform distributions of continuous values exhibit common means when the range of permissible parameter values is bounded [32]. Similarly as with the mean itself, Figs. 6(*c*) and 6(*d*) find that the *mean difference* among the ordered parameter values is loosely correlated for the bistable spring stiffness but strongly correlated for the bistable spring span, which supports the prior conclusions.

Figure 5 plots the statistics of the design variable (*a*) range, (*b*) mean, and (*c*) ordered difference for all individuals of the final generation as produced by the GA. The horizontal axes show the respective statistics computed for the bistable spring stiffnesses, whereas the vertical axes are those statistics for the bistable spring spans. Each data point is the statistic computed for one of the 100 individuals of the final generation and the data point shading varies from light to dark for increasing fitness of the individual. From this evaluation throughout Figs. 5(*a*)–5(*c*), the concentrations of parameter values for the bistable spring spans (i.e., concentrations along vertical axes), notably for higher-fitness individuals, exemplify that particular range, mean, and mean difference among the ordered spring span design variables of the six module metastructure are needed to ensure that the stable equilibria are as equally spaced apart as possible. In contrast, the assessment in Figs. 5(*a*)–5(*c*) verifies the observation from Fig. 6 that the bistable spring stiffness value selection is not as important toward achieving this particular performance objective. Therefore, by the utilization of the GA in such a novel, statistical manner, important insights may be derived to make design decisions that result in the sought-after performance and properties adaptivity of multimodule metastructures.

6.2 Designing Metastructures With Equally Incremented Reaction Force Levels. Then, considering the second performance measure, the GA is programmed to optimize the mechanical properties by pursuing an equal spacing between adjacent reaction force levels of a multimodule metastructure when the global end displacement is prescribed, illustrated for clarity in the bottom left panel of Fig. 5. In other words, for any global end displacement of z_0 where multiple metastable states occur, the GA aims to identify a metastructure design having adjacent reaction forces equally spaced by a consistent force increment ΔF. The design variables and GA settings are the same as those described above, and the results of the algorithm for a six-module metastructure are shown in Fig. 7. In contrast to simply achieving equidistant stable

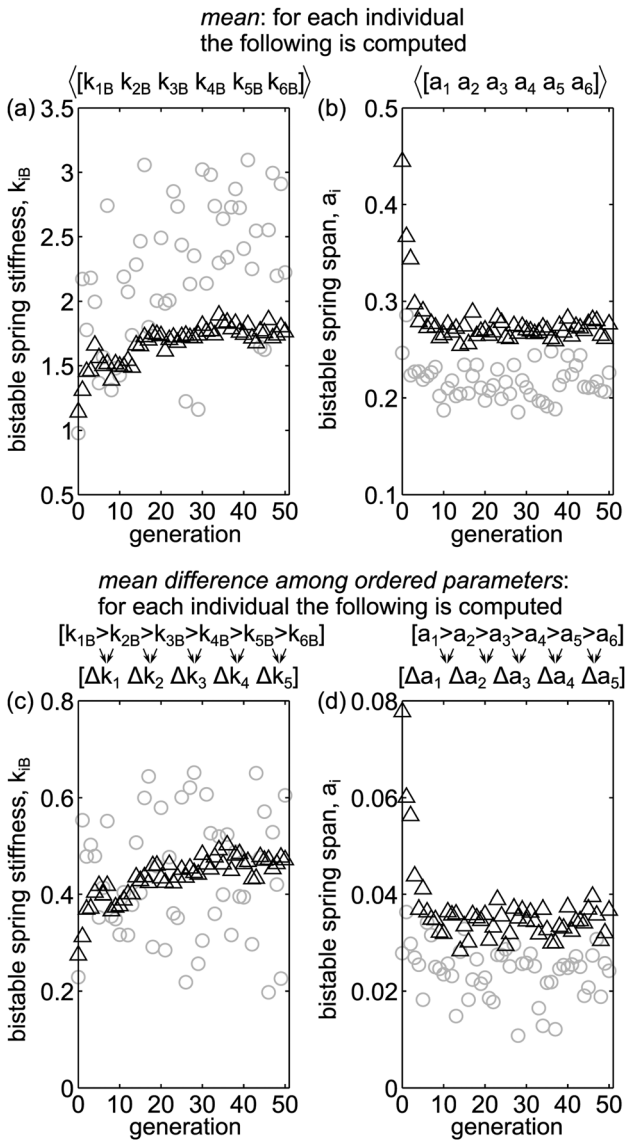

Fig. 6 GA results for equidistant stable equilibria. Design variable statistics, showing triangles as the mean statistics for a given generation whereas circles are the statistics according to the best-fit individual of that generation. (*a*) The mean of the six bistable spring stiffnesses, (*b*) the mean of the six bistable spring spans, (*c*) the mean difference among the ordered values of bistable spring stiffness and the corresponding statistic in (*d*) for the bistable spring span.

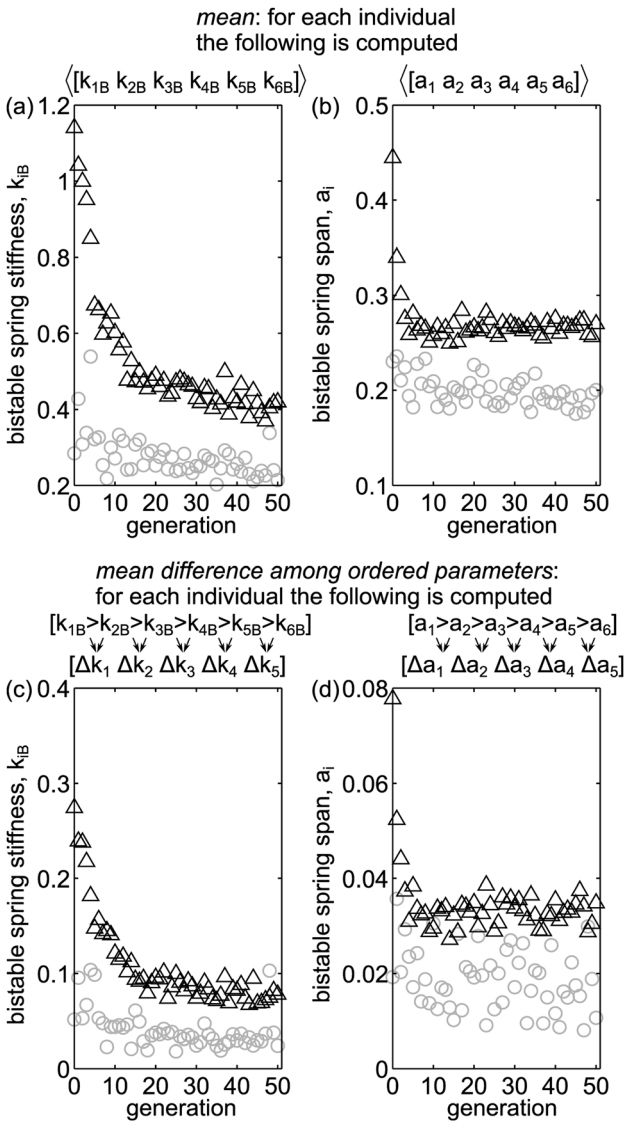

Fig. 7 GA results for equally spaced reaction force levels. Design variable statistics, showing triangles as the mean statistics for a given generation whereas circles are the statistics according to the best-fit individual of that generation. (*a*) The mean of the six bistable spring stiffnesses, (*b*) the mean of the six bistable spring spans, (*c*) the mean difference among the ordered values of bistable spring stiffness and the corresponding statistic in (*d*) for the bistable spring span.

equilibria, the findings in Fig. 7 indicate that both the bistable spring span and the bistable spring stiffness are essential design variables to strategically select toward realizing equally incremented levels of metastructure reaction force. Figures 7(*a*) and 7(*b*) show that the generation mean values of the bistable spring stiffness and span, respectively, both converge to respective values as the GA optimization proceeds. Likewise, the results of Figs. 7(*c*) and 7(*d*) find that the ordered parameters are also required to exhibit certain mean differences, as evidenced by the statistical convergence of the generation mean values over the course of the GA evolutionary computations. Figures 5(*d*)–5(*f*) present the set of statistics produced by the final GA generation toward achieving equally spaced reaction forces across the range of end displacement for which multiple forces are possible. The higher performing individuals (darker shaded data) of this last generation are seen to cluster to particular statistical regimes for both design variables in agreement with the overall evolutionary results shown in Fig. 7. These results indicate that the selection of bistable spring stiffnesses k_{iB} and spans a_i, among the six modules of a given metastructure, must comply with particular statistical properties in order to achieve the preferred equal spacing between adjacent reaction forces. Thus, more stringent design variable control is needed to realize this performance measure when compared to the design variable sensitivities involved toward effecting equidistant stable equilibria.

6.3 Influence of the Number of Assembled Metastable Modules. The findings in Secs. 6.1 and 6.2 elucidate the roles of two key design variables toward achieving target properties adaptivity or topological variation in six-module metastructures. Yet, it may be asked how general such conclusions are, namely, whether they are extensible to metastructures assembled from any number of metastable modules. To assess such an influence of scalability, the second performance metric of equally spaced levels of reaction force is re-evaluated by the GA, considering

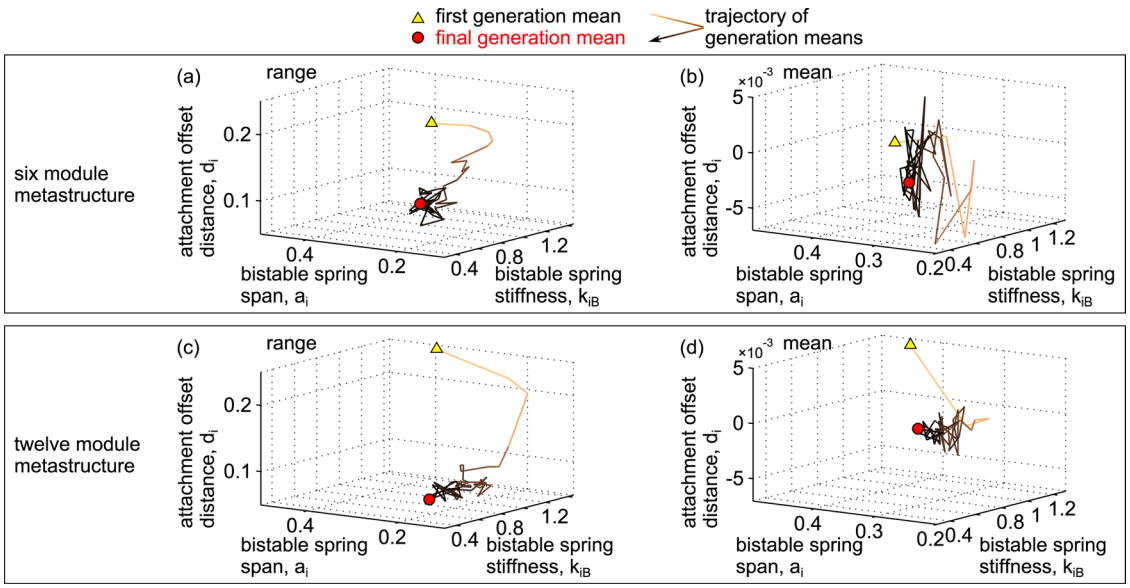

Fig. 8 Generation mean design variable statistics over the course of 50 evolutionary generations. Shading from light to dark shows increasing generation number. Results in (*a*) and (*b*) are for the six module metastructure while those in (*c*) and (*d*) are for the twelve module metastructure. In (*a*) and (*c*) are the design variable ranges, while (*b*) and (*d*) show the design variable means.

six- and twelve-module metastructure platforms. Based on preliminary results, it was determined to introduce an additional design variable to the optimization routine, namely, the attachment offset distance d_i, while the GA algorithm again considered 100 individuals in each of 50 evolutionary generations.

Figures 8(*a*) and 8(*b*) plot the values of the design statistics for the range and mean, respectively, of the mean generation result for the six-module metastructure, while Figs. 8(*c*) and 8(*d*) present the corresponding data for the twelve-module metastructure. The shading of the line from first (triangle) to last (circle) generation is indicated by increasing darkness to highlight the trajectory of the GA over the course of the evolutionary routine. It is seen that the strategic selection of bistable spring stiffnesses and spans plays an appreciable role toward realizing this performance metric for the six module platform. This is evident in Figs. 8(*a*) and 8(*b*) based on the observation that the statistics for the range and mean values of bistable spring stiffness and span converge as the GA routine proceeds, while in contrast the attachment offset distance statistics exhibit poor consistency in value from one generation to the next (i.e., much greater variation in the trajectories in the vertical axis).

Yet, considering the findings for the twelve module metastructure as shown in Figs. 8(*c*) and 8(*d*), a different conclusion may be drawn. In fact, from these results, the role of the attachment offset distance is apparent since the GA trajectories exhibit undeniable convergence in the statistics for all three design variables. Because the final generation mean values of the statistics for the bistable spring stiffness and span are nearly identical when comparing the six- and twelve-module metastructures, the role of the number of assembled modules is therefore to introduce an important, new design variable influence in terms of the attachment offset distance. Collectively, the discoveries of this section reveal important sensitivities of multimodule metastructure design toward achieving performance measures, such as prescribed stable topological change and preferred adaptation in reaction force by transitioning among the many metastable states. Although the concept of utilizing an assembly of metastable modules to create metastructures may potentially introduce an open-ended design problem, it is found that strategic design variable selection—in a *statistical* sense—is an effective means to realize target adaptation performance. Future efforts of this research will pursue further insights on the interplay between statistics and design as it relates to the development of modular metastructures possessing target performance and functionality.

7 Final Remarks and Conclusions

The design concept presented here suggests that great potential is affected by the assembly of metastable modules into mechanical metastructures. This paper presents one exemplary realization of a fully functional (i.e., adaptable) module, but it is recognized that combining a bistable spring/elasticity in series with an additional non-negative stiffness spring/elasticity has many possible module-based embodiments. This includes magnetoelastic interactions within structural materials [33] or architected material systems [34–36], and material-type building blocks with voids [8]. These recent innovations exploit *periodic* designs and the potential for internal instabilities in the periodic arrangements to result in macroscopic adaptivity. In contrast, the approach established here is to design the modules at the local level to facilitate a prescribed global synergy in performance and functionality once thereafter assembled. By the design investigation of Sec. 6, it is seen that this method facilitates macroscopic features in a rational way useful for engineering design purposes. Nevertheless, through continuing investigations the authors are taking inspiration from the recent, related works [8,33–36] to design multidimensional metastructures based on the concepts established here. In the ongoing work, parallel and series configurations of metastable modules are being explored so as to empower multiple working macroscopic dimensions with target characteristics, e.g., large continuous shape change, large stiffness adaptation, etc.

In summary, this investigation shows that modularity in an assembled structural system invests direct means to create and harness the metastable states of metastructures for programmable properties adaptivity. Experimental and analytical results exemplify that near-continuous properties adaptivity and stable topology change are effected as the number of assembled modules increases. The measurements also uncover opportunities to realize adjustable hysteresis (hence, energy dissipation) by harnessing the vast number of metastable states. Although the development of multimodule metastructures poses interesting design-based challenges, the incorporation of the analytical model into a novel GA routine demonstrates that the achievement of target *global* metastructure performance characteristics are met for preferred statistical distributions of key design variables at the *local* level, thereby closing the open-endedness of the design problem and guiding future assembly strategies. Altogether, this research shows that a

new concept using building blocks having an essential variation of mechanical properties (coexisting metastable states) promotes enhanced and synergistic adaptivity via assembled, modular metastructures which leverage design variable heterogeneities to achieve target performance measures.

Acknowledgment

The authors gratefully acknowledge the support of the Air Force Office of Scientific Research (FA9550-13-1-0122) under the administration of Dr. David Stargel and the University of Michigan Collegiate Professorship.

References

[1] Wagg, D., Bond, I., Weaver, P., and Friswell, M., 2007, *Adaptive Structures: Engineering Applications*, Wiley, Chichester, UK.
[2] Shim, J., Shan, S., Košmrlj, A., Kang, S. H., Chen, E. R., Weaver, J. C., and Bertoldi, K., 2013, "Harnessing Instabilities for Design of Soft Reconfigurable Auxetic/Chiral Materials," Soft Matter, **9**(34), pp. 8198–8202.
[3] Schenk, M., and Guest, S. D., 2013, "Geometry of Miura-Folded Metamaterials," Proc. Natl. Acad. Sci., **110**(9), pp. 3276–3281.
[4] Crivaro, A., Sheridan, R., Frecker, M., Simpson, T. W., and von Lockette, P., 2014, "Bistable Compliant Mechanisms Using Magneto Active Elastomer Actuation," ASME Paper No. DETC2014-35007.
[5] Nicolaou, Z. G., and Motter, A. E., 2012, "Mechanical Metamaterials With Negative Compressibility Transitions," Nat. Mater., **11**(7), pp. 608–613.
[6] Celli, P., and Gonella, S., 2015, "Tunable Directivity in Metamaterials With Reconfigurable Cell Symmetry," Appl. Phys. Lett., **106**(9), p. 091905.
[7] Fuchi, K., Buskohl, P. R., Joo, J. J., Reich, G. W., and Vaia, R. A., 2015, "Resonance Tuning of RF Devices Through Origami Folding," 20th International Conference on Composite Materials, Copenhagen, Denmark, pp. 1–10.
[8] Florijn, B., Coulais, C., and van Hecke, M., 2014, "Programmable Mechanical Metamaterials," Phys. Rev. Lett., **113**(17), p. 175503.
[9] Silverberg, J. L., Na, J. H., Evans, A. A., Liu, B., Hull, T. C., Santangelo, C. D., Lang, R. J., and Hayward, R. C., and Cohen, I., 2015, "Origami Structures With a Critical Transition to Bistability Arising From Hidden Degrees Of Freedom," Nat. Mater., **14**(4), pp. 389–393.
[10] Shan, S., Kang, S. H., Wang, P., Qu, C., Shian, S., Chen, E. R., and Bertoldi, K., 2014, "Harnessing Multiple Folding Mechanisms in Soft Periodic Structures for Tunable Control of Elastic Waves," Adv. Funct. Mater. **24**(31), pp. 4935–4942.
[11] Wang, P., Casadei, F., Shan, S., Weaver, J. C., and Bertoldi, K., 2014, "Harnessing Buckling to Design Tunable Locally Resonant Acoustic Metamaterials," Phys. Rev. Lett., **113**(1), p. 014301.
[12] Kuder, I. K., Arrieta, A. F., Rathier, W. E., and Ermanni, P., 2013, "Variable Stiffness Material and Structural Concepts for Morphing Applications," Prog. Aerosp. Sci., **63**, pp. 33–55.
[13] Dai, F., Li, H., and Du, S., 2013, "A Multi-Stable Lattice Structures and Its Snap-Through Behavior Among Multiple States," Compos. Struct., **97**, pp. 56–63.
[14] Daynes, S., Trask, R. S., and Weaver, P. M., 2014, "Bio-Inspired Structural Bistability Employing Elastomeric Origami for Morphing Applications," Smart Mater. Struct., **23**(12), p. 125011.
[15] Bowen, L., Springsteen, K., Feldstein, H., Frecker, M., Simpson, T. W., and von Lockette, P., 2015, "Development and Validation of a Dynamic Model of Magneto-Active Elastomer Actuation of the Origami Waterbomb Base," J. Mech. Robots, **7**(1), p. 011010.
[16] Li, S., and Wang, K. W., 2015, "Fluidic Origami With Embedded Pressure Dependent Multi-Stability: A Plant Inspired Innovation," J. R. Soc. Interface, **12**(111), p. 20150639.
[17] Wu, Z., Harne, R. L., and Wang, K. W., 2015, "Exploring a Modular Adaptive Metastructure Concept Inspired by Muscle's Cross-Bridge," J. Intell. Mater. Syst. Struct., (online).
[18] Lakes, R. S., and Drugan, W. J., 2002, "Dramatically Stiffer Elastic Composite Materials Due to a Negative Stiffness Phase?," J. Mech. Phys. Solids, **50**(5), pp. 979–1009.
[19] Fritzen, F., and Kochmann, D. M., 2014, "Material Instability-Induced Extreme Damping in Composites: A Computational Study," Int. J. Solids Struct., **51**, pp. 4101–4112.
[20] Caruel, M., Allain, J. M., and Truskinovsky, L., 2013, "Muscle as a Metamaterial Operating Near a Critical Point," Phys. Rev. Lett., **110**(24), p. 248103.
[21] Schenk, M., and Guest, S. D., 2014, "On Zero Stiffness," Proc. Inst. Mech. Eng., Part C, **228**(10), pp. 1701–1714.
[22] Puglisi, G., and Truskinovsky, L., 2002, "A Mechanism of Transformational Plasticity," Continuum Mech. Thermodyn., **14**(5), pp. 437–457.
[23] Holst, G. L., Teichert, G. H., and Jensen, B. D., 2011, "Modeling and Experiments of Buckling Modes and Deflection of Fixed-Guided Beams in Compliant Mechanisms," ASME J. Mech. Des., **133**(5), p. 051002.
[24] Chen, Y. H., and Lan, C. C., 2012, "An Adjustable Constant-Force Mechanism for Adaptive End-Effector Operations," ASME J. Mech. Des., **134**(3), p. 031005.
[25] Kovacic, I., and Brennan, M. J., eds., 2011, *The Duffing Equation: Nonlinear Oscillators and Their Behaviour*, Wiley, Chichester, UK.
[26] Barbarino, S., Saavedra Flores, E. I., Ajaj, R. M., Dayyani, I., and Friswell, M. I., 2014, "A Review on Shape Memory Alloys With Applications to Morphing Aircraft," Smart Mater. Struct., **23**(6), p. 063001.
[27] Kidambi, N., Harne, R. L., and Wang, K. W., 2016, "Adaptation of Energy Dissipation in a Mechanical Metastable Module Excited Near Resonance," ASME J. Vib. Acoust., **138**, p. 011001.
[28] Romeo, F., Sigalov, G., Bergman, L. A., and Vakakis, A. F., 2015, "Dynamics of a Linear Oscillator Coupled to a Bistable Light Attachment: Numerical Study," ASME J. Comput. Nonlinear Dyn., **10**, p. 011007.
[29] Biggs, N. L., 1979, "The Roots of Combinatorics," Hist. Math., **6**(2), pp. 109–136.
[30] Antoniadis, I., Chronopoulos, D., Spitas, V., and Koulocheris, D., 2015, "Hyper-Damping Peroperties of a Stiff and Stable Linear Oscillator With a Negative Stiffness Element," J. Sound Vib., **346**, pp. 37–52.
[31] Haupt, R. L., and Haupt, S. E., 1998, *Practical Genetic Algorithms*, Wiley, Hoboken, NJ.
[32] Freund, R. J., Wilson, W. J., and Mohr, D. L., 2010, *Statistical Methods*, Academic Press, Burlington, MA.
[33] Schaeffer, M., and Ruzzene, M., 2015, "Wave Propagation in Multistable Magneto-Elastic Lattices," Int. J. Solids Struct., **56–57**, pp. 78–95.
[34] Tipton, C. R., Han, E., and Mullin, T., 2012, "Magneto-Elastic Buckling of a Soft Cellular Solid," Soft Matter, **8**(26), pp. 6880–6883.
[35] Shan, S., Kang, S. H., Raney, J. R., Wang, P., Fang, L., Candido, F., Lewis, J. A., and Bertoldi, K., 2015, "Multistable Architected Materials for Trapping Elastic Strain Energy," Adv. Mater., **27**(29), pp. 4296–4301.
[36] Rafsanjani, A., Akbarzadeh, A., and Pasini, D., 2015, "Snapping Mechanical Metamaterials Under Tension," Adv. Mater., **27**(39), pp. 5931–5935.